

Volume Enclosed by Subdivision Surfaces with Sharp Creases

by Jan Hakenberg, Ulrich Reif, Scott Schaefer, Joe Warren

published on viXra.org - June 10th, 2014

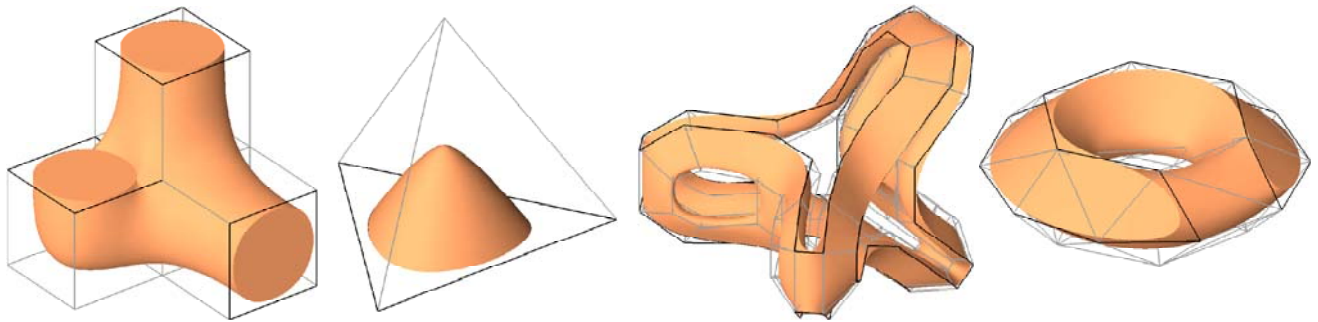


Figure: Four unit cubes glued together with the three cycles as sharp creases define a Catmull-Clark subdivision surface that encloses a volume of 2.9615786... The exact value is a fraction with 1558 digits. The tetrahedron with all edges of length 1 and one triangle boundary as crease defines a Loop subdivision surface that encloses a volume of $\frac{9835279661079132863588159}{228340616075693288629862400\sqrt{2}}$. Our formula also applies to more complex meshes with creases. The volume of the torus control mesh contracts to that of the Loop surface by a factor of 0.836059... ■

Abstract

Subdivision surfaces with sharp creases are used in surface modeling and animation. The framework that derives the volume formula for classic surface subdivision also applies to the crease rules. After a general overview, we turn to the popular Catmull-Clark, and Loop algorithms with sharp creases. We enumerate common topology types of facets adjacent to a crease. We derive the trilinear forms that determine their contribution to the global volume. The mappings grow in complexity as the vertex valence increases. In practice, the explicit formulas are restricted to meshes with a certain maximum valence of a vertex.

The first author dedicates this work to the memory of Andrew Ladd, Nik Sperling, and Leif Dickmann. The article and additional resources are available at www.hakenberg.de. The first author was partially supported by personal savings accumulated during his visit to the Nanyang Technological University as a visiting research scientist in 2012-2013. He'd like to thank everyone who worked to make this opportunity available to him.

Introduction

Surface subdivision schemes are tuned to produce surfaces that appear smooth everywhere. Creases are a simple extension that provide the option to model sharp features in the surface. Across the crease, the surface normal is generally not continuous, as can be seen in the illustration above.

[Hoppe et al. 1994] extend the Loop subdivision scheme to handle sharp creases. [DeRose et al. 1998] present refinement of creases in Catmull-Clark meshes. The concept is the same in both algorithms: Along an edge cycle of the mesh that is designated as crease, cubic B-spline subdivision rules for curves apply. In particular, control points that are not part of the crease cycle do not affect the refinement of the crease. In the limit, the

crease is identical to a cubic B-spline curve.

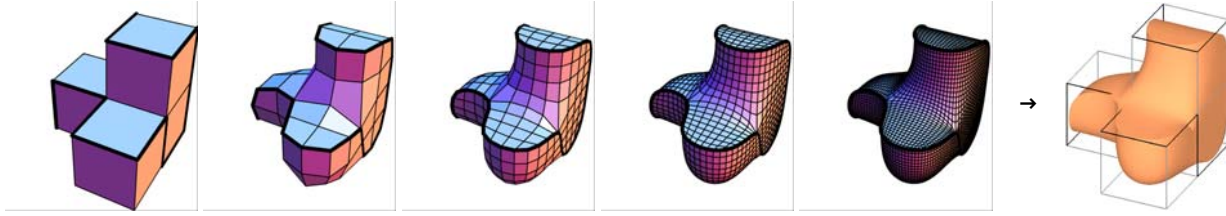


Figure: Four iterations of the Catmull-Clark subdivision scheme applied to an initial mesh of four unit cubes glued together. The bolded edge cycle is defined as a sharp crease. We prove that the limit surface encloses a volume of 3.274816588... The exact value is a fraction with 1369 digits, see [Hakenberg 2014]. ■

An early use of sharp creases in subdivision surfaces was to model the fingernails of the character *Geri* in Pixar's 1997 short film *Geri's game*. From then on, subdivision with creases has been a tool in surface modeling, and frequently used in animations, [Autodesk 2013].

The volume enclosed by a Catmull-Clark, and Loop surface is derived in [Hakenberg et al. 2014]. We simply work out the implications of crease subdivision rules in this article. The framework requires us to derive a collection of trilinear forms for the control points of a quad, or a triangular facet that is adjacent to a crease. A trilinear form computes the volume contribution of a single facet, which is added up over all facets to the global volume. The computation is efficient, since at most one round of subdivision of the mesh is required to yield the volume enclosed by the limit surface.

Possible applications of our formula are 1) the design of surfaces with sharp creases to enclose a specific volume, and 2) the deformation of surfaces subject to volume preservation.

The article is structured as follows: We recap the volume formula for subdivision surfaces as derived in [Hakenberg et al. 2014]. We elaborate on the implications for facets that are affected by crease subdivision rules. Then, we derive the volume contribution for the most relevant local mesh topologies of facets adjacent to creases in a Catmull-Clark, and Loop mesh.

Background

For stationary subdivision schemes with certain additional properties, the enclosed volume of the subdivision surface defined by a closed, orientable mesh M is determined by a collection of trilinear forms, see [Hakenberg et al. 2014]. The subdivision surface is partitioned by facets $f \in M$, where the surface corresponding to a facet f is completely determined by a set of control points (px_i, py_i, pz_i) for $i = 1, 2, \dots, m(f)$ in the neighborhood of facet f . The volume contribution of a facet f is a trilinear form applied to the coordinates of the $m(f)$ control points. The total volume is the sum of the contributions of all facets. In particular,

$$\text{vol}(M) = \sum_{f \in M} \text{vol}(f) = \sum_{f \in M} \sum_{i,j,k}^{m(f)} (A_{i,j,k}^{\tau(f)} - A_{i,k,j}^{\tau(f)}) px_i py_j pz_k = \sum_{f \in M} \sum_{i,j,k}^{m(f)} Y_{i,j,k}^{\tau(f)} px_i py_j pz_k$$

where $A_{i,j,k}^{\tau(f)}$, and $Y_{i,j,k}^{\tau(f)} := A_{i,j,k}^{\tau(f)} - A_{i,k,j}^{\tau(f)}$ are trilinear forms of dimension $m(f) \times m(f) \times m(f)$. We abbreviate

$\sum_{i,j,k}^m X(i, j, k) := \sum_{i=1}^m \sum_{j=1}^m \sum_{k=1}^m X(i, j, k)$. The coefficients $A_{i,j,k}^{\tau(f)}$ depend only on the subdivision rules that determine the surface corresponding to the topology $\tau(f)$ of facet f , and are obtained by solving a system of linear equations. Once the collection of trilinear forms $Y^{\tau(f)}$ is established for a subdivision scheme, the formula applies to any closed, orientable mesh M .

An example for the characterization of the topology type $\tau(f)$ of a facet is the valence of the non-regular vertex.

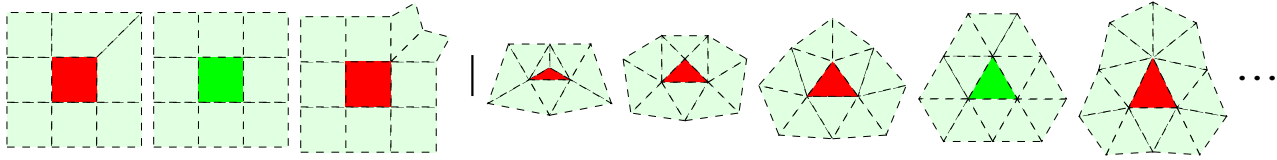


Figure: For Catmull-Clark, a facet f is a quad of the one-time subdivided initial mesh. For Loop, a facet f is a triangle of the one-time subdivided initial mesh. $m(f)$ is the number of vertices in the one-ring of f . The one-ring completely defines the surface across the facet f . ■

When the surface associated to a facet f is affected by the subdivision rules along creases, a trilinear form different from the surface case contributes in the volume formula.

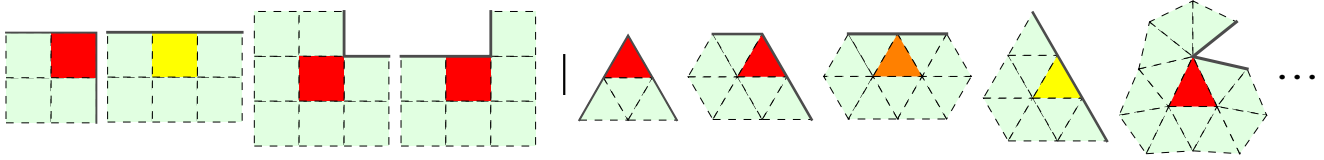


Figure: Facets adjacent to a sharp crease in a Catmull-Clark, and Loop mesh together with the control points that determine the surface across the facet. The crease edges are indicated by a thick line. Vertices on the “other side” of the sharp crease do not affect the surface associated to the facet. ■

The guiding principle to obtain the coefficients is that the volume formula has to be invariant under one round of subdivision of the mesh, i.e. $\text{vol}(M) = \text{vol}(S(M))$, since that operation does not change the limit surface. The careful choice of the partition with the facets allows to reduce the equation to $\text{vol}(f) = \sum_h \text{vol}(f_h)$, where the facets f_h constitute the decomposition of f by subdivision. The conservation of volume under subdivision is also a useful criteria for detecting possible mistakes in an implementation of the formula. A surface subdivision scheme S typically partitions a facet f into 4 smaller facets $S(f) \rightarrow \{f_1, f_2, f_3, f_4\}$ in the refined mesh, which is what we assume henceforth to keep the notation reasonable.

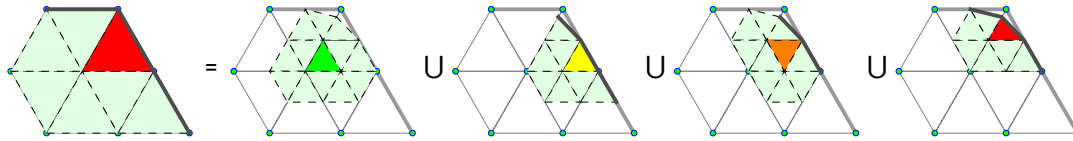


Figure: Refinement of a triangular facet f into 4 smaller facets f_h for $h \in \{1, 2, 3, 4\}$ in a Loop mesh. The facet is adjacent to a crease. The topology types of the refined facets $\tau(f_h)$ are pairwise different, but $\tau(f) = \tau(f_4)$. ■

Subdivision of the control points of facet f to the control points of f_h is a coordinatewise, linear mapping that we express as the matrix S^h with dimension $m(f_h) \times m(f)$ for $h \in \{1, 2, 3, 4\}$. Considering all products $px_i py_j pz_k$ as a basis, we obtain a total of $m(f)^3$ equations

$$A_{i,j,k}^{\tau(f)} = \sum_{a,b,c}^{m(f_1)} A_{a,b,c}^{\tau(f_1)} S_{a,i}^1 S_{b,j}^1 S_{c,k}^1 + \sum_{a,b,c}^{m(f_2)} A_{a,b,c}^{\tau(f_2)} S_{a,i}^2 S_{b,j}^2 S_{c,k}^2 + \sum_{a,b,c}^{m(f_3)} A_{a,b,c}^{\tau(f_3)} S_{a,i}^3 S_{b,j}^3 S_{c,k}^3 + \sum_{a,b,c}^{m(f_4)} A_{a,b,c}^{\tau(f_4)} S_{a,i}^4 S_{b,j}^4 S_{c,k}^4$$

for all $i, j, k = 1, 2, \dots, m(f)$. We denote the system of linear equations by $L(\tau(f); \tau(f_1), \tau(f_2), \tau(f_3), \tau(f_4))$.

The approach to solve for unknown coefficients $A_{i,j,k}^{\tau(f)}$ in L depends on the rhs:

- *regular*. When $\tau(f) = \tau(f_h)$ for all $h \in \{1, 2, 3, 4\}$, the linear system L is homogeneous. Then, the coefficients $A_{i,j,k}^{\tau(f)}$ have to be identified in the nullspace of a matrix. The derivation of the volume form $Y^{\tau(f)}$ generally involves calibration. The regular case is not required subsequently in the article. Examples can instead be found in [Hakenberg et al. 2014]. We color regular facets in green.
- *semi-regular*. When $\tau(f) = \tau(f_3) = \tau(f_4)$, and $A^{\tau(f_1)}$ and $A^{\tau(f_2)}$ are known, the equations L constitute a non-homogeneous linear system. We color semi-regular facets in yellow.

- *non-regular*: When $\tau(f) = \tau(f_4)$, and $A^{\tau(f_h)}$ are known for $h \in \{1, 2, 3\}$. We use the colors red, and orange to indicate facets of non-regular topology. Additional examples can be found in [Hakenberg et al. 2014].
- *explicit*: When $\tau(f) \neq \tau(f_h)$ and $A^{\tau(f_h)}$ are known for all $h \in \{1, 2, 3, 4\}$, then $A^{\tau(f)}$ follows by explicit computation. A facet of this topology type is assigned yet a different color.

In all except the explicit case, the nullspace of the matrix of L has to be investigated to characterize the solution space of $Y^{\tau(f)}$. For the non-regular case, we shall make use of a result from [Hakenberg et al. 2014], which is reworded here for convenience:

Lemma 1: Let matrix S^4 have eigenvalue 1 with multiplicity 1, and all other eigenvalues be of absolute value < 1 . Then, the nullspace of L is 1-dimensional and projects to 0, when computing $Y_{i,j,k}^{\tau(f)} := A_{i,j,k}^{\tau(f)} - A_{i,k,j}^{\tau(f)}$. ■

[Hakenberg et al. 2014] show that the collection of trilinear forms $Y^{\tau(f)}$ are *not* uniquely determined for the Catmull-Clark, and the Loop scheme. However, any solution $A^{\tau(f)}$ of the linear system L projects to a unique alternating form $\hat{Y}_{i,j,k}^{\tau(f)}$ when averaging all signed permutations of $Y^{\tau(f)}$

$$\hat{Y}_{i,j,k}^{\tau(f)} = \frac{1}{6} \left(Y_{i,j,k}^{\tau(f)} - Y_{i,k,j}^{\tau(f)} + Y_{j,k,i}^{\tau(f)} - Y_{j,i,k}^{\tau(f)} + Y_{k,i,j}^{\tau(f)} - Y_{k,j,i}^{\tau(f)} \right) \quad \text{for } i, j, k = 1, 2, \dots, m(f).$$

Applications

The Catmull-Clark subdivision scheme is published as [Catmull/Clark 1978]. The Loop scheme is introduced in [Loop 1987]. The subdivision rules along crease edge cycles in a mesh are illustrated in the following.

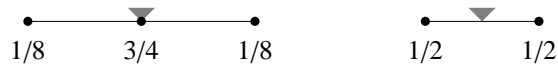


Figure: One round of cubic B-spline subdivision for curves consists of vertex repositioning, and mid-edge vertex insertion. ■

We derive the volume formula for Catmull-Clark, and Loop subdivision surfaces with sharp creases. Due to the uniqueness of the coefficients $\hat{Y}_{i,j,k}^{\tau(f)}$, we shall derive the trilinear form of the volume contribution of a facet in the alternating form. We require that crease cycles are pairwise disjoint, i.e. non-intersecting. The adaptation to handle meshes with *dart*, and *corner* vertices is discussed as future work. A quad, or triangle facet f is *adjacent to a crease* if one, or more vertices of the quad, or triangle also belong to a crease edge cycle. The volume contribution of a facet f that is not adjacent to a crease is determined by a trilinear form $\hat{Y}^{\tau(f)}$ already derived in [Hakenberg et al. 2014].

When f is adjacent to a crease, we denote the topology type by a tuple $n.m$. The first number n is the valence of the non-regular vertex (that also belongs to the crease). The second number m enumerates different configurations of the crease. All topology types are illustrated graphically. The subdivision weights are integer fractions.

That means we can establish the trilinear forms $\hat{Y}^{\tau(f)}$ in exact, symbolical notation. However, as the valence of the non-regular crease vertex increases, the volume forms become more difficult to establish because of computer memory constraints. The coefficients are available for download from www.hakenberg.de.

For all subsequent non-regular topology types, the matrix S^4 has the eigenvalue structure required for the application of Lemma 1. That means the uniqueness of the alternating form is asserted without the need to inspect the nullspace of the matrix in L .

We illustrate numerous examples of subdivision surfaces with sharp creases in a separate publication, [Hakenberg 2014]. The mesh specifications, and results therein can help to validate other implementations of the volume formula.

Catmull-Clark with sharp creases

A facet f that is not adjacent to a crease is assigned a topology type $\tau(f) \in \{3, 4, 5, 6, \dots\}$ according to the valence of the non-regular vertex, or $\tau(f) = 4$ if facet f is regular.

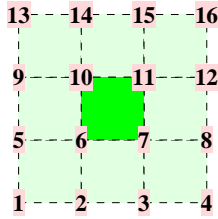


Figure: A quad facet f of regular topology $\tau(f) = 4$ in a Catmull-Clark mesh with the $m(f) = 16$ control points from the one-ring. ■

One round of subdivision of a facet f adjacent to a crease results in one or more regular facets, for instance $\tau(f_1) = 4$. That means in the linear system L , the form A^4 from [Hakenberg et al. 2014] is required for the derivation of the volume form. Furthermore, we begin the derivation for $\tau(f) = 2.1$, since the topology type is a by-product of subdividing facets adjacent to creases of types $\tau(f) \in \{1.1, 3.2, 4.2, \dots\}$, where $A^{2.1}$ is required.

Topology type 2.1 (semi-regular)

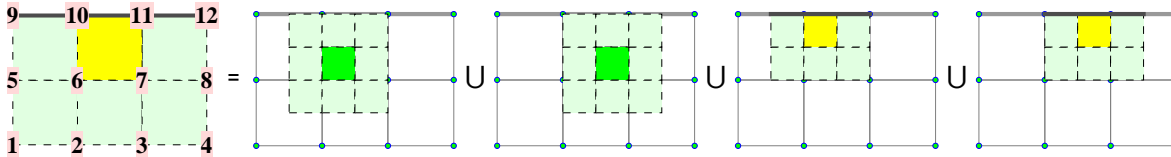


Figure: One round of subdivision of a facet f of topology type $\tau(f) = 2.1$ results in 4 smaller facets f_h with $\tau(f_1) = \tau(f_2) = 4$, and $\tau(f_3) = \tau(f_4) = 2.1$. The surface associated to f is determined by $m(f) = 12$ control points. ■

In addition to the equations $L(2.1; 4, 4, 2.1, 2.1)$, we impose the obvious symmetries $A_{i,j,k}^{2.1} + A_{\sigma(i),\sigma(j),\sigma(k)}^{2.1} = 0$ for all $i, j, k = 1, 2, \dots, 12$ where $\sigma(1) = 4, \sigma(2) = 3, \sigma(3) = 2, \dots, \sigma(11) = 10$, and $\sigma(12) = 9$ is a mirror operation. The 3-dimensional nullspace of the combined linear system can be calculated symbolically. We verify that no vector from the nullspace contributes to the alternating trilinear form $\hat{Y}^{2.1}$.

Example: $\hat{Y}_{1,6,10}^{2.1} = \frac{6985}{18289152}, \hat{Y}_{2,8,11}^{2.1} = \frac{20269}{38102400}, \hat{Y}_{3,9,12}^{2.1} = -\frac{1027}{76204800}, \hat{Y}_{4,5,9}^{2.1} = -\frac{11}{18289152}, \hat{Y}_{6,9,12}^{2.1} = -\frac{90613}{457228800}$. ■

Topology type 1.1

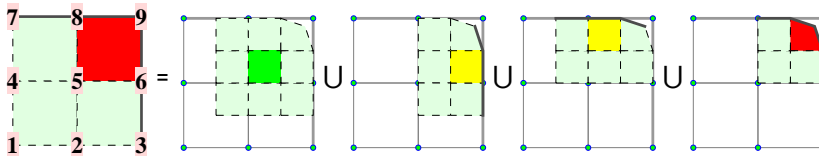


Figure: Subdivision of a facet f with $\tau(f) = 1.1$ results in $\tau(f_1) = 4, \tau(f_2) = \tau(f_3) = 2.1$, and $\tau(f_4) = 1.1$. The surface associated to f is determined by $m(f) = 9$ control points. ■

We state the subdivision matrices S^h that map the control points of facet f coordinatewise to those of f_h for $h \in \{1, 2, 3, 4\}$. S^1 is a 16×9 matrix, S^2 and S^3 have dimension 12×9 , and S^4 is square 9×9 .

$$\begin{aligned}
 S^1 &= \frac{1}{64} \begin{pmatrix} 16 & 16 & 0 & 16 & 16 & 0 & 0 & 0 & 0 \\ 4 & 24 & 4 & 4 & 24 & 4 & 0 & 0 & 0 \\ 0 & 16 & 16 & 0 & 16 & 16 & 0 & 0 & 0 \\ 4 & 4 & 0 & 24 & 24 & 0 & 4 & 4 & 0 \\ 1 & 6 & 1 & 6 & 36 & 6 & 1 & 6 & 1 \\ 0 & 4 & 4 & 0 & 24 & 24 & 0 & 4 & 4 \\ 0 & 0 & 8 & 0 & 0 & 48 & 0 & 0 & 8 \\ 0 & 0 & 0 & 16 & 16 & 0 & 16 & 16 & 0 \\ 0 & 0 & 0 & 4 & 24 & 4 & 4 & 24 & 4 \\ 0 & 0 & 0 & 0 & 16 & 16 & 0 & 16 & 16 \\ 0 & 0 & 0 & 0 & 0 & 32 & 0 & 0 & 32 \\ 0 & 0 & 0 & 0 & 0 & 0 & 32 & 32 & 0 \\ 0 & 0 & 0 & 0 & 0 & 0 & 8 & 48 & 8 \\ 0 & 0 & 0 & 0 & 0 & 0 & 0 & 32 & 32 \\ 0 & 0 & 0 & 0 & 0 & 8 & 0 & 8 & 48 \end{pmatrix}, & S^2 &= \frac{1}{64} \begin{pmatrix} 0 & 0 & 0 & 0 & 0 & 0 & 8 & 48 & 8 \\ 0 & 0 & 0 & 4 & 24 & 4 & 4 & 24 & 4 \\ 1 & 6 & 1 & 6 & 36 & 6 & 1 & 6 & 1 \\ 4 & 24 & 4 & 4 & 24 & 4 & 0 & 0 & 0 \\ 0 & 0 & 0 & 0 & 0 & 0 & 0 & 32 & 32 \\ 0 & 0 & 0 & 0 & 16 & 16 & 0 & 16 & 16 \\ 0 & 4 & 4 & 0 & 24 & 24 & 0 & 4 & 4 \\ 0 & 16 & 16 & 0 & 16 & 16 & 0 & 0 & 0 \\ 0 & 0 & 0 & 0 & 8 & 0 & 8 & 48 \\ 0 & 0 & 0 & 0 & 0 & 32 & 0 & 0 & 32 \\ 0 & 0 & 8 & 0 & 0 & 48 & 0 & 0 & 8 \\ 0 & 0 & 32 & 0 & 0 & 32 & 0 & 0 & 0 \end{pmatrix}, & S^3 &= \frac{1}{64} \begin{pmatrix} 4 & 4 & 0 & 24 & 24 & 0 & 4 & 4 & 0 \\ 1 & 6 & 1 & 6 & 36 & 6 & 1 & 6 & 1 \\ 0 & 4 & 4 & 0 & 24 & 24 & 0 & 4 & 4 \\ 0 & 0 & 8 & 0 & 0 & 48 & 0 & 0 & 8 \\ 0 & 0 & 0 & 16 & 16 & 0 & 16 & 16 & 0 \\ 0 & 0 & 0 & 4 & 24 & 4 & 4 & 24 & 4 \\ 0 & 0 & 0 & 0 & 16 & 16 & 0 & 16 & 16 \\ 0 & 0 & 0 & 0 & 0 & 32 & 0 & 0 & 32 \\ 0 & 0 & 0 & 0 & 0 & 0 & 32 & 32 & 0 \\ 0 & 0 & 0 & 0 & 0 & 0 & 8 & 48 & 8 \\ 0 & 0 & 0 & 0 & 0 & 0 & 0 & 32 & 32 \\ 0 & 0 & 0 & 0 & 0 & 0 & 8 & 0 & 8 & 48 \end{pmatrix}, \\
 S^4 &= \frac{1}{64} \begin{pmatrix} 1 & 6 & 1 & 6 & 36 & 6 & 1 & 6 & 1 \\ 0 & 4 & 4 & 0 & 24 & 24 & 0 & 4 & 4 \\ 0 & 0 & 8 & 0 & 0 & 48 & 0 & 0 & 8 \\ 0 & 0 & 0 & 4 & 24 & 4 & 4 & 24 & 4 \\ 0 & 0 & 0 & 0 & 16 & 16 & 0 & 16 & 16 \\ 0 & 0 & 0 & 0 & 0 & 32 & 0 & 0 & 32 \\ 0 & 0 & 0 & 0 & 0 & 8 & 48 & 8 \\ 0 & 0 & 0 & 0 & 0 & 0 & 32 & 32 \\ 0 & 0 & 0 & 0 & 8 & 0 & 8 & 48 \end{pmatrix}.
 \end{aligned}$$

The indexing means $S^4_{7,8} = \frac{48}{64}$. The eigenvalues of S^4 are $1, \frac{1}{2}, \frac{1}{4}, \dots, \frac{1}{64}$ in descending order. Lemma 1 asserts that the linear system $L(1.1; 4, 2.1, 2.1, 1.1)$ defines $\hat{Y}^{1.1}$ uniquely.

Example: $\hat{Y}^{1.1}_{1,4,8} = -\frac{12913}{198132480}, \hat{Y}^{1.1}_{2,3,7} = \frac{11}{254016}, \hat{Y}^{1.1}_{4,5,6} = \frac{28664707}{1435717483200}, \hat{Y}^{1.1}_{5,6,9} = \frac{302808242662819}{8009014933119200}$. ■

Topology type 3.1

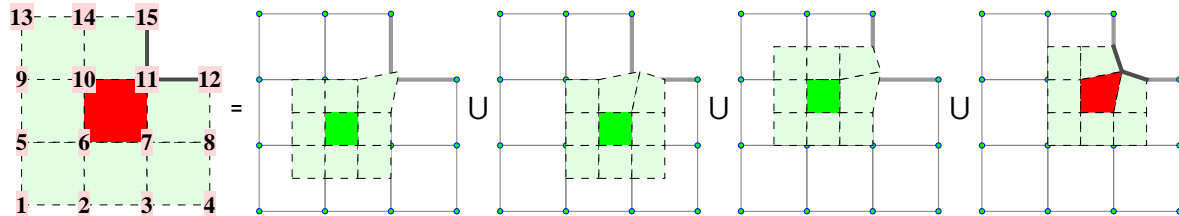


Figure: Decomposition of a facet f with $\tau(f) = 3.1$ results in $\tau(f_1) = \tau(f_2) = \tau(f_3) = 4$, and $\tau(f_4) = 3.1$; $m(f) = 15$. ■

The linear system $L(3.1; 4, 4, 4, 3.1)$ defines $\hat{Y}^{3.1}$ uniquely.

Example: $\hat{Y}^{3.1}_{1,2,10} = \frac{91324698848626238240330396076991308024065498141}{902494031699009693429525497232067947003635206727680}$. ■

Topology type 3.2

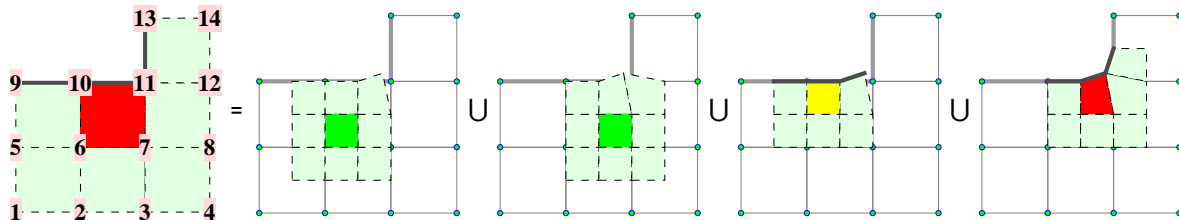


Figure: Subdivision of a facet f with $\tau(f) = 3.2$; $m(f) = 14$. ■

The linear system $L(3.2; 4, 4, 2.1, 3.2)$ defines $\hat{Y}^{3.2}$ uniquely.

Example: $\hat{Y}_{1,3,11}^{3,2} = \frac{3754899360452115120948509}{71808793287635553429051313920}$, $\hat{Y}_{2,4,5}^{3,2} = \frac{5}{2286144}$, $\hat{Y}_{3,5,9}^{3,2} = -\frac{55}{1306368}$. ■

Topology type 4.1

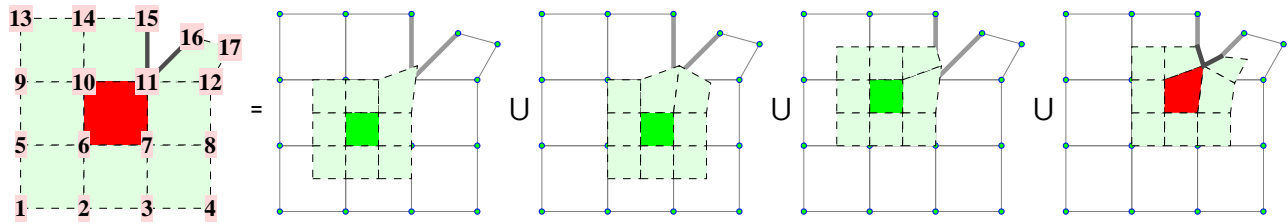


Figure: Decomposition of a facet f with $\tau(f) = 4.1$; $m(f) = 17$. ■

The linear system $L(4.1; 4, 4, 4, 4.1)$ determines $\hat{Y}^{4.1}$ uniquely.

Example: $\hat{Y}_{1,3,15}^{4.1} = \frac{332859298055844612698638290644680067}{433813079667636289625706022029625498982400}$, $\hat{Y}_{2,4,13}^{4.1} = \frac{5}{219469824}$. ■

Topology type 4.2

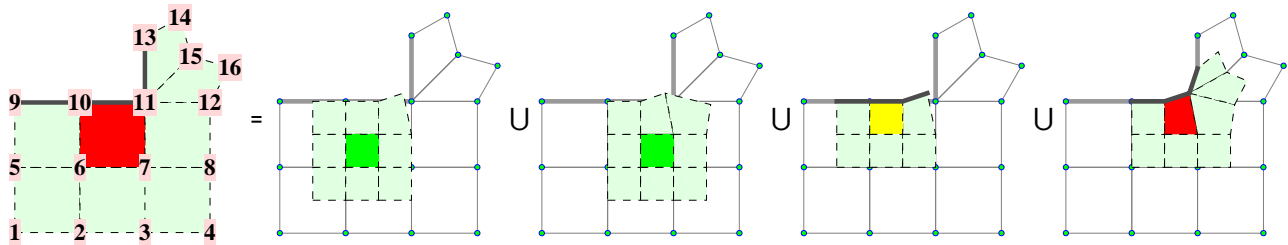


Figure: Decomposition of a facet f with $\tau(f) = 4.2$; $m(f) = 16$. ■

The linear system $L(4.2; 4, 4, 2.1, 4.2)$ defines $\hat{Y}^{4.2}$ uniquely.

Example: $\hat{Y}_{1,3,14}^{4.2} = \frac{8512340234545396400}{44785435264516019862423664921143}$, $\hat{Y}_{2,4,9}^{4.2} = \frac{5}{3048192}$. ■

Topology type 5.1

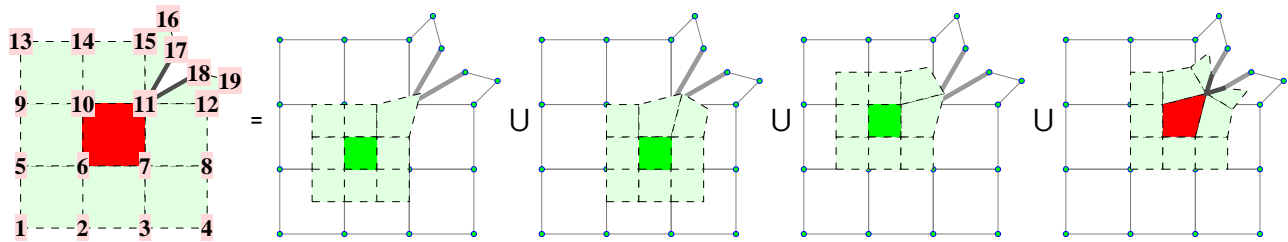


Figure: Decomposition of a facet f with $\tau(f) = 5.1$; $m(f) = 19$. ■

The linear system $L(5.1; 4, 4, 4, 5.1)$ defines $\hat{Y}^{5.1}$ uniquely.

Example: $\hat{Y}_{1,2,6}^{5.1} = \frac{25321142767366766979276702659645686531891465171}{180460214658619244851639459245884670391729343170560}$, $\hat{Y}_{2,3,13}^{5.1} = \frac{397}{731566080}$. ■

Topology type 5.2

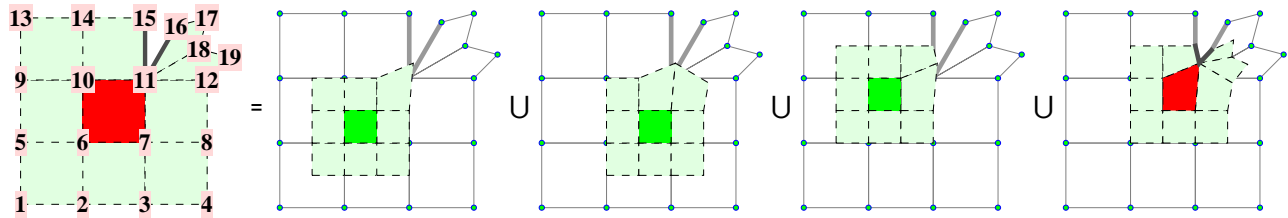


Figure: Decomposition of a facet f with $\tau(f) = 5.2$; $m(f) = 19$. ■

The linear system $L(5.2; 4, 4, 4, 5.2)$ defines $\hat{Y}^{5.2}$ uniquely.

Example: $\hat{Y}_{1,2,8}^{5.2} = \frac{32\,208\,349\,702\,482\,915\,328\,214\,993\,889\,747\,969\,814\,150\,871}{50\,754\,435\,372\,736\,662\,614\,523\,597\,912\,905\,063\,547\,673\,877\,766\,720}$. ■

Topology type 5.3

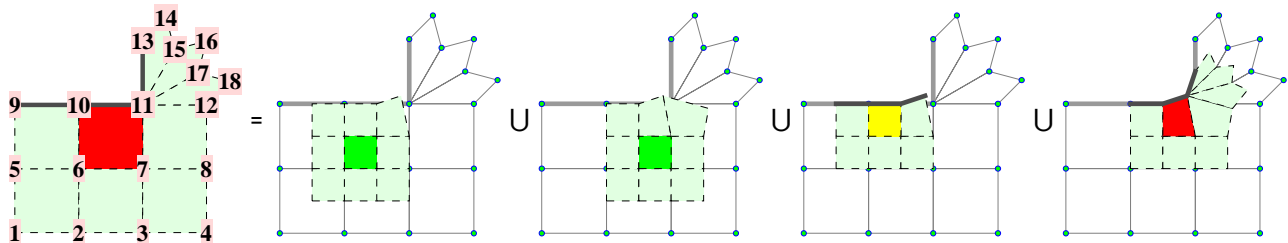


Figure: Decomposition of a facet f with $\tau(f) = 5.3$; $m(f) = 18$. ■

The linear system $L(5.3; 4, 4, 2.1, 5.3)$ defines $\hat{Y}^{5.3}$ uniquely.

Example: $\hat{Y}_{1,4,18}^{5.3} = \frac{131\,450\,484\,823\,813\,732\,545\,338\,913\,915\,392\,725\,339}{537\,083\,972\,198\,271\,562\,058\,450\,771\,565\,132\,947\,594\,432\,568\,960}$, $\hat{Y}_{1,5,18}^{5.3} = -\frac{16\,766\,977}{212\,522\,446\,547\,841\,780}$. ■

Summary

The previous sections enumerate all possible topology types of facets adjacent to a sharp crease with valence ≤ 5 in a Catmull-Clark mesh.

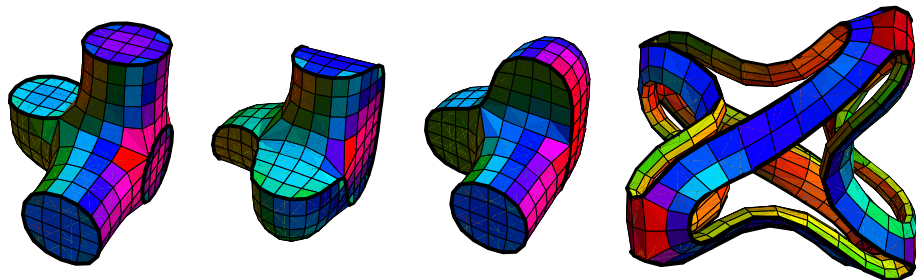
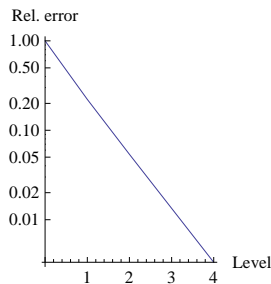


Figure: Typical approximation rate of the volume enclosed by the mesh at different levels of subdivision to the volume of the limit surface obtained by our new formula. 2 rounds of subdivision seem to achieve slightly more than 1 digit of decimal precision. Right: Facets are colored based on their volume contribution. ■

To establish the volume enclosed by a quad mesh, the surface spanned by a possibly non-planar quad $q \in M$ is parameterized using the bilinear basis functions $B_1(s, t) = (1 - s, 1 - t)$, $B_2(s, t) = (s, 1 - t)$, $B_3(s, t) = (s, t)$, and $B_4(s, t) = (1 - s, t)$ over the domain $[0, 1] \times [0, 1]$. The volume contribution of q is determined by the alternating trilinear form \hat{Y}^q with dimension $4 \times 4 \times 4$, and entries defined by $\hat{Y}_{1,2,3}^q = \hat{Y}_{1,2,4}^q = \hat{Y}_{1,3,4}^q = \hat{Y}_{2,3,4}^q = \frac{1}{12}$.

Loop with sharp creases

A facet f that is not adjacent to a crease is of topology type $\tau(f) \in \{3, 4, 5, 6, 7, \dots\}$. The number $\tau(f)$ denotes the valence of the non-regular vertex, or $\tau(f) = 6$ if facet f is regular.

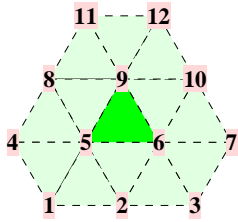


Figure: A triangular facet f of regular topology $\tau(f) = 6$ in a Loop mesh with the $m(f) = 12$ control points from the one-ring. ■

One round of subdivision of a facet f adjacent to a crease results in one or more regular facets, for instance $\tau(f_1) = 6$. That means in the linear system L , the form A^6 from [Hakenberg et al. 2014] is required for the derivation of the volume form. The case $\tau(f) = 1.2$ is an exception. Furthermore, we begin the derivation with $\tau(f) = 3.1$, and $\tau(f) = 3.2$, since these types are a by-product of subdividing facets of many other topology types adjacent to a crease, where $A^{3.1}$, and $A^{3.2}$ are required.

Topology type 3.1

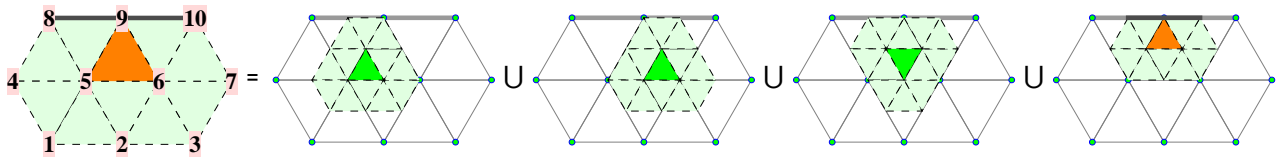


Figure: One round of subdivision of a facet f of topology type $\tau(f) = 3.1$ results in four smaller facets f_h with $\tau(f_1) = \tau(f_2) = \tau(f_3) = 6$, and $\tau(f_4) = 3.1$. The surface associated to f is determined by $m(f) = 10$ control points. ■

The eigenvalues of S^4 are $1, \frac{1}{2}, \frac{1}{2}, \frac{1}{4}, \dots, \frac{1}{16}$ in descending order. Lemma 1 asserts that the linear system $L(3.1; 6, 6, 6, 3.1)$ determines $\hat{Y}^{3.1}$ uniquely.

Example: $\hat{Y}_{1,2,6}^{3.1} = \frac{67}{217728}, \hat{Y}_{1,7,9}^{3.1} = \frac{149}{4435200}, \hat{Y}_{2,6,7}^{3.1} = -\frac{14207}{23950080}, \hat{Y}_{4,7,9}^{3.1} = \frac{1021}{59875200}, \hat{Y}_{5,8,10}^{3.1} = -\frac{191437}{59875200}$. ■

Topology type 3.2 (semi-regular)

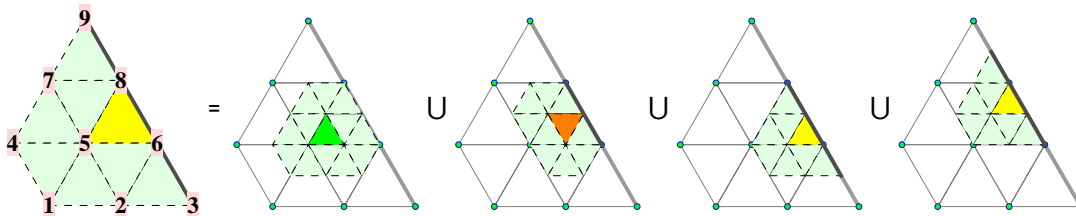


Figure: Subdivision of a facet f with $\tau(f) = 3.2$ results in $\tau(f_1) = 6, \tau(f_2) = 3.1$, and $\tau(f_3) = \tau(f_4) = 3.2$. The surface associated to f is determined by $m(f) = 9$ control points. ■

In addition to $L(3.2; 6, 3.1, 3.2, 3.2)$, we impose the obvious symmetries $A_{i,j,k}^{3.2} + A_{\sigma(i),\sigma(j),\sigma(k)}^{3.2} = 0$ for all $i, j, k = 1, 2, \dots, 9$ where $\sigma(1) = 4, \sigma(2) = 7, \sigma(3) = 9, \dots, \sigma(8) = 6$, and $\sigma(9) = 3$ is a mirror operation. The 3-dimensional nullspace of the combined linear system can be calculated symbolically. We verify that no vector from the nullspace contributes to the alternating trilinear form $\hat{Y}^{3.2}$.

Example: $\hat{Y}_{1,2,4}^{3,2} = \frac{227}{120960}$, $\hat{Y}_{1,5,7}^{3,2} = \frac{199}{362880}$, $\hat{Y}_{2,4,8}^{3,2} = -\frac{727}{1088640}$, $\hat{Y}_{3,6,9}^{3,2} = -\frac{97}{725760}$, $\hat{Y}_{4,5,8}^{3,2} = \frac{3041}{2177280}$, $\hat{Y}_{5,7,9}^{3,2} = -\frac{149}{311040}$. ■

Topology type 1.1 (explicit)

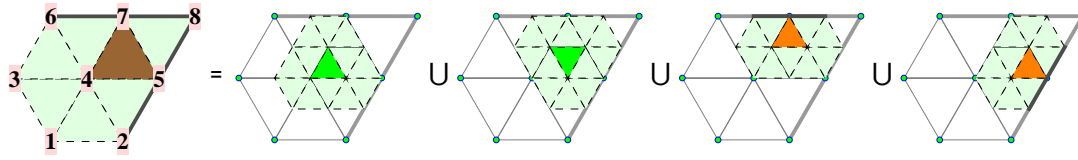


Figure: Decomposition of a facet f with $\tau(f) = 1.1$ results in $\tau(f_1) = \tau(f_2) = 6$, and $\tau(f_3) = \tau(f_4) = 3.1$; $m(f) = 8$. ■

Evaluation of the rhs of $L(1.1; 6, 6, 3.1, 3.1)$ gives $A^{1.1}$. The form $\hat{Y}^{1.1}$ follows uniquely.

Example: $\hat{Y}_{1,2,3}^{1.1} = \frac{1}{22680}$, $\hat{Y}_{1,4,6}^{1.1} = \frac{673}{1088640}$, $\hat{Y}_{1,5,7}^{1.1} = \frac{799}{544320}$, $\hat{Y}_{2,3,8}^{1.1} = -\frac{143}{2177280}$, $\hat{Y}_{3,4,6}^{1.1} = \frac{101}{136080}$. ■

Topology type 1.2

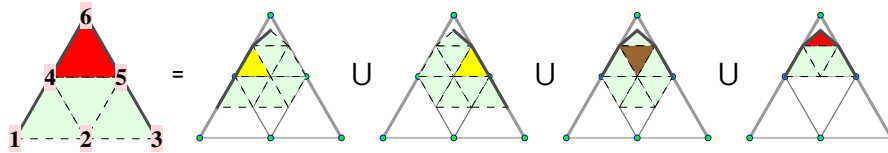


Figure: Subdivision of a facet f with $\tau(f) = 1.2$; $m(f) = 6$. ■

We state the subdivision matrices S^h that map the control points of facet f coordinatewise to those of f_h for $h \in \{1, 2, 3, 4\}$. S^1 and S^2 have dimension 9×6 , S^3 is a 8×6 matrix, and S^4 is square 6×6 .

$$S^1 = \frac{1}{8} \begin{pmatrix} 0 & 0 & 1 & 0 & 6 & 1 \\ 0 & 0 & 0 & 0 & 4 & 4 \\ 0 & 0 & 0 & 1 & 1 & 6 \\ 0 & 3 & 1 & 1 & 3 & 0 \\ 0 & 1 & 0 & 3 & 3 & 1 \\ 0 & 0 & 0 & 4 & 0 & 4 \\ 1 & 3 & 0 & 3 & 1 & 0 \\ 1 & 0 & 0 & 6 & 0 & 1 \\ 4 & 0 & 0 & 4 & 0 & 0 \end{pmatrix}, S^2 = \frac{1}{8} \begin{pmatrix} 1 & 3 & 0 & 3 & 1 & 0 \\ 0 & 3 & 1 & 1 & 3 & 0 \\ 0 & 0 & 4 & 0 & 4 & 0 \\ 1 & 0 & 0 & 6 & 0 & 1 \\ 0 & 1 & 0 & 3 & 3 & 1 \\ 0 & 0 & 1 & 0 & 6 & 1 \\ 0 & 0 & 0 & 4 & 0 & 4 \\ 0 & 0 & 0 & 4 & 0 & 4 \\ 0 & 0 & 0 & 1 & 1 & 6 \end{pmatrix}, S^3 = \frac{1}{8} \begin{pmatrix} 0 & 3 & 1 & 1 & 3 & 0 \\ 0 & 0 & 1 & 0 & 6 & 1 \\ 1 & 3 & 0 & 3 & 1 & 0 \\ 0 & 1 & 0 & 3 & 3 & 1 \\ 0 & 0 & 0 & 0 & 4 & 4 \\ 1 & 0 & 0 & 6 & 0 & 1 \\ 0 & 0 & 0 & 4 & 0 & 4 \\ 0 & 0 & 0 & 4 & 0 & 4 \\ 0 & 0 & 0 & 1 & 1 & 6 \end{pmatrix}, S^4 = \frac{1}{8} \begin{pmatrix} 1 & 0 & 0 & 6 & 0 & 1 \\ 0 & 1 & 0 & 3 & 3 & 1 \\ 0 & 0 & 1 & 0 & 6 & 1 \\ 0 & 0 & 0 & 4 & 0 & 4 \\ 0 & 0 & 0 & 1 & 1 & 6 \end{pmatrix}.$$

The eigenvalues of S^4 are $1, \frac{1}{2}, \frac{1}{4}, \dots, \frac{1}{8}$ in descending order. Lemma 1 asserts that the linear system $L(1.2; 3.2, 3.2, 1.1, 1.2)$ determines $\hat{Y}^{1.2}$ uniquely.

Example: $\hat{Y}_{1,2,6}^{1.2} = \frac{1}{576}$, $\hat{Y}_{1,3,5}^{1.2} = \frac{7}{51840}$, $\hat{Y}_{1,5,6}^{1.2} = \frac{151}{30240}$, $\hat{Y}_{2,3,4}^{1.2} = \frac{67}{120960}$, $\hat{Y}_{2,4,6}^{1.2} = -\frac{67}{6048}$, $\hat{Y}_{3,4,5}^{1.2} = -\frac{731}{181440}$. ■

Topology type 1.3 (explicit)

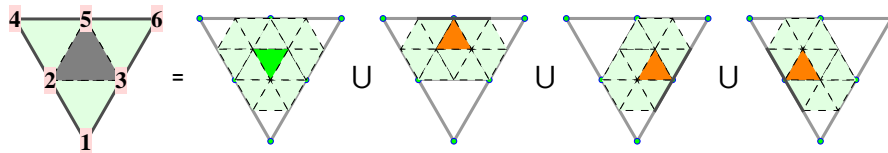


Figure: Decomposition of a facet f with $\tau(f) = 1.3$ results in $\tau(f_1) = 6$, and $\tau(f_2) = \tau(f_3) = \tau(f_4) = 3.1$; $m(f) = 6$. ■

The topology type $\tau(f) = 1.3$ exists in a mesh at most until depth 1 of the subdivision iteration. In other words, the derivation is not required if the mesh is subdivided twice before applying the volume formula.

Evaluation of the rhs of $L(1.3; 6, 3.1, 3.1, 3.1)$ gives $A^{1.3}$. The form $\hat{Y}^{1.3}$ follows uniquely.

Example: $\hat{Y}_{1,3,5}^{1.3} = \frac{757}{90720}$, $\hat{Y}_{1,3,6}^{1.3} = -\frac{181}{181440}$, $\hat{Y}_{2,3,5}^{1.3} = \frac{1439}{45360}$, $\hat{Y}_{2,4,6}^{1.3} = -\frac{127}{36288}$, $\hat{Y}_{3,5,6}^{1.3} = -\frac{5}{378}$, $\hat{Y}_{4,5,6}^{1.3} = \frac{181}{181440}$. ■

Topology type 2.1

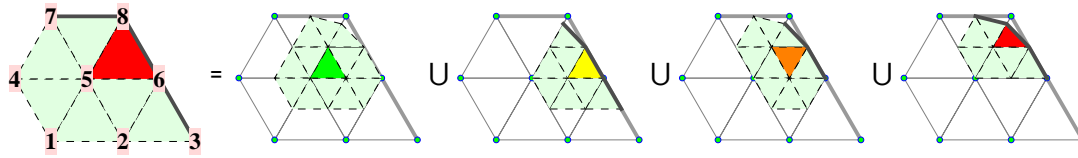


Figure: Decomposition of a facet f with $\tau(f) = 2.1$; $m(f) = 8$. ■

The linear system $L(2.1; 6, 3.2, 3.1, 2.1)$ determines $\hat{Y}^{2.1}$ uniquely.

Example: $\hat{Y}_{1,2,7}^{2.1} = \frac{137}{725760}$, $\hat{Y}_{2,4,5}^{2.1} = -\frac{40971011}{75433897728}$, $\hat{Y}_{3,5,8}^{2.1} = -\frac{7220411}{1587859200}$, $\hat{Y}_{3,6,8}^{2.1} = -\frac{5604080861}{2828771164800}$. ■

Topology type 4.1

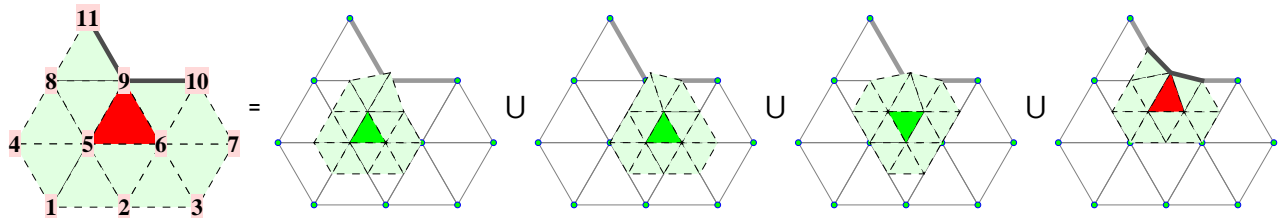


Figure: Decomposition of a facet f with $\tau(f) = 4.1$; $m(f) = 11$. ■

The linear system $L(4.1; 6, 6, 6, 4.1)$ determines $\hat{Y}^{4.1}$ uniquely.

Example: $\hat{Y}_{1,3,9}^{4.1} = \frac{522868883}{8346648784320}$, $\hat{Y}_{2,7,11}^{4.1} = \frac{504092267076477455722079009363}{47913934497945582619195419645792000}$. ■

Topology type 4.2

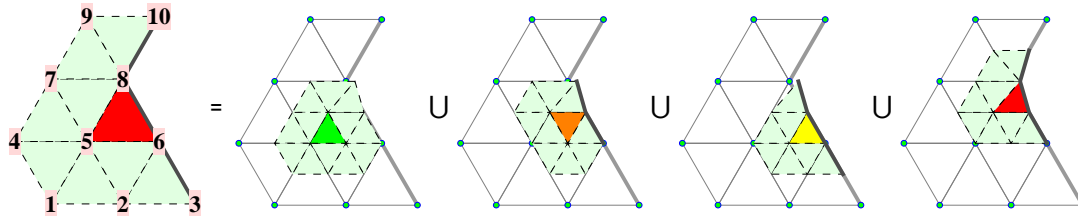


Figure: Decomposition of a facet f with $\tau(f) = 4.2$; $m(f) = 10$. ■

The linear system $L(4.2; 6, 3.1, 3.2, 4.2)$ determines $\hat{Y}^{4.2}$ uniquely.

Example: $\hat{Y}_{1,6,9}^{4.2} = \frac{8853569889285284305621256471025331}{421581229745912359601811050175011977500}$, $\hat{Y}_{2,3,10}^{4.2} = \frac{370343273447318357}{14551956103113525669120}$. ■

Topology type 5.1

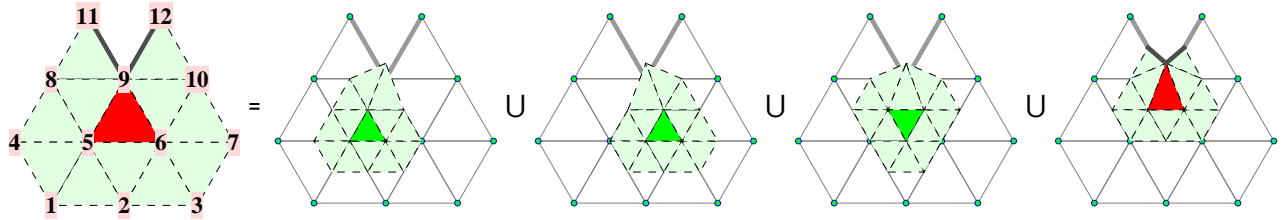


Figure: Decomposition of a facet f with $\tau(f) = 5.1$; $m(f) = 12$. ■

The linear system $L(5.1; 6, 6, 6, 5.1)$ determines $\hat{Y}^{5.1}$ uniquely.

Example: $\hat{Y}_{1,11,12}^{5.1} = -\frac{1706662770105731828005269146671663339}{1460887459608929115708832369326065169312672}$. ■

Topology type 5.2

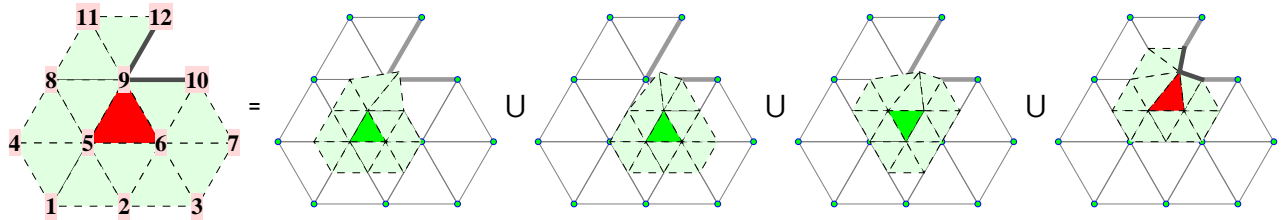


Figure: Decomposition of a facet f with $\tau(f) = 5.2$; $m(f) = 12$. ■

The linear system $L(5.2; 6, 6, 6, 5.2)$ determines $\hat{Y}^{5.2}$ uniquely.

Example: $\hat{Y}_{3,10,12}^{5.2} = \frac{982766755119695968574706305980646912107779497}{174641540921099212463849672648392576197168634924800}$. ■

Topology type 5.3

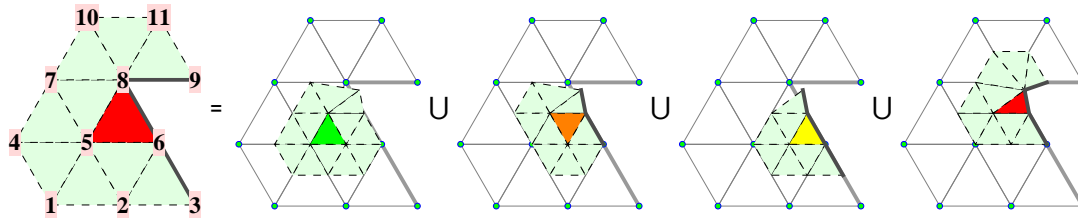


Figure: Decomposition of a facet f with $\tau(f) = 5.3$; $m(f) = 11$. ■

The linear system $L(5.3; 6, 3.1, 3.2, 5.3)$ determines $\hat{Y}^{5.3}$ uniquely.

Example: $\hat{Y}_{1,6,9}^{5.3} = \frac{2707579102925448432697949601438619512151}{72794430656157428099632868836478913533318400}$. ■

Topology type 6.1

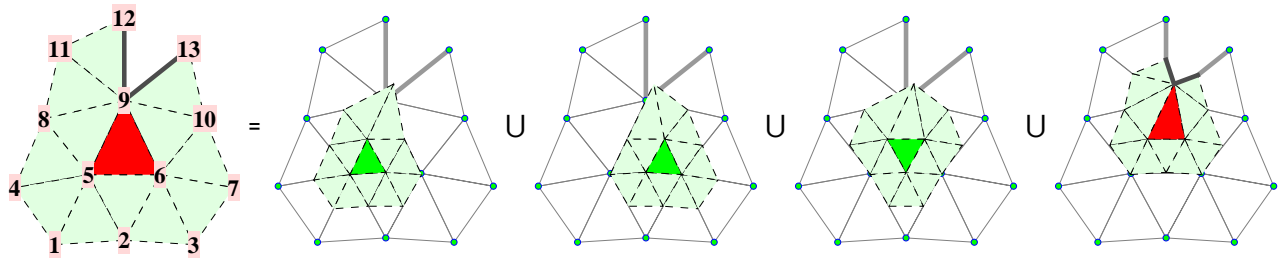


Figure: Decomposition of a facet f with $\tau(f) = 6.1$; $m(f) = 13$. ■

The linear system $L(6.1; 6, 6, 6, 6.1)$ determines $\hat{Y}^{6.1}$ uniquely.

Example: $\hat{Y}_{3,8,12}^{6.1} = -\frac{2770410521268316209419372341445587617299}{520212230956067771371169696610297718215561600}$. ■

Topology type 6.2

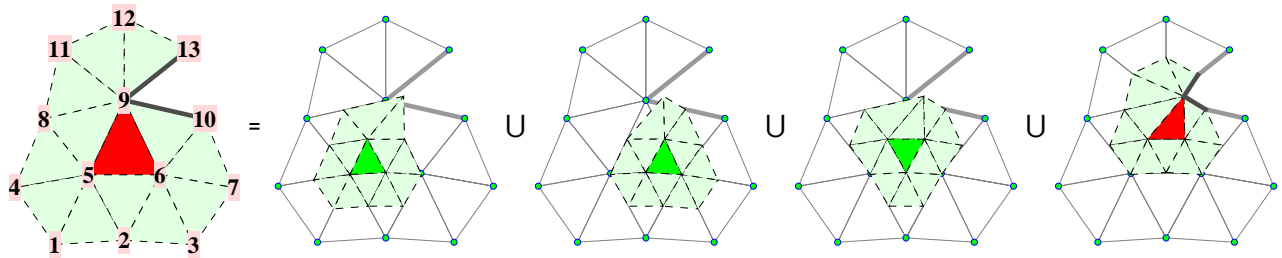


Figure: Decomposition of a facet f with $\tau(f) = 6.2$; $m(f) = 13$. ■

The linear system $L(6.2; 6, 6, 6, 6.2)$ determines $\hat{Y}^{6.2}$ uniquely.

Example: $\hat{Y}_{1,9,12}^{6.2} = \frac{369936151051443519138798531725497047884083}{1364401445531083172883086570633504515260657888000}$. ■

Topology type 6.3

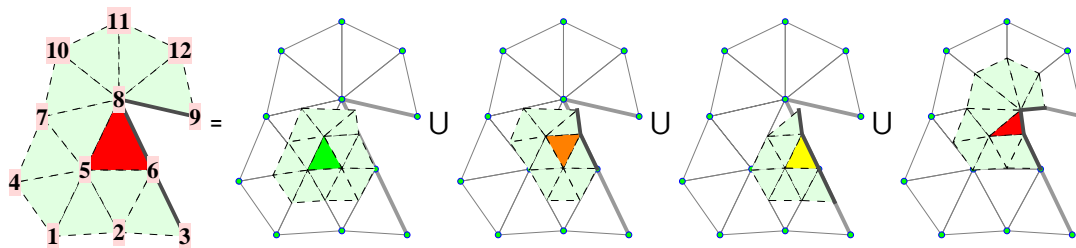


Figure: Decomposition of a facet f with $\tau(f) = 6.3$; $m(f) = 12$. ■

The linear system $L(6.3; 6, 6, 6, 6.3)$ determines $\hat{Y}^{6.3}$ uniquely.

Example: $\hat{Y}_{2,8,10}^{6.3} = \frac{3788836092953000361574059231745228390306399}{40632051474754871606203561158147350726434111875}$. ■

Summary

The previous sections enumerate all possible topology types of a triangular facet adjacent to a crease with valence ≤ 6 in a Loop mesh.

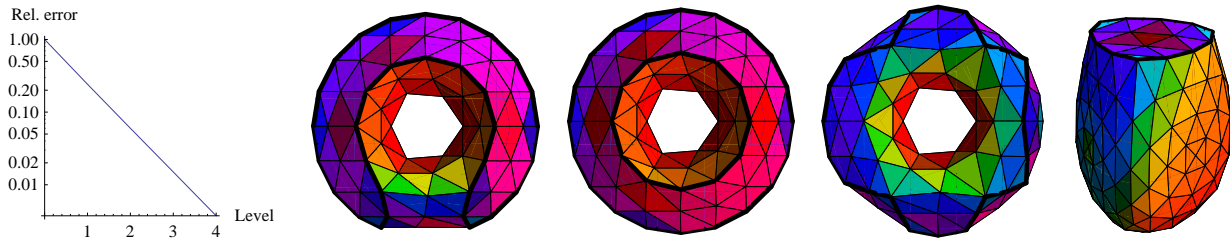


Figure: Typical approximation rate of the volume enclosed by the piecewise linear mesh at different levels of subdivision to the volume of the limit surface obtained by our new formula. 2 rounds of subdivision seem to achieve slightly more than 1 digit of decimal precision. Right: Facets are colored based on their contribution to the global volume. ■

Future work

We have derived the alternating trilinear forms for facets adjacent to sharp creases that are required to compute the volume enclosed by the subdivision surface. The forms are available up to a certain valence of the non-regular vertex. In the future, trilinear forms for greater valences may be computed.

The discussion in our article is restricted to meshes with pairwise disjoint crease cycles. [Hoppe et al. 1994] incorporates two other possibilities: 1) A *dart* vertex is at the start (and end) of a sharp crease that is non-cyclic. Ordinary surface subdivision rules apply at dart vertices. 2) A *corner* vertex is where two, or more creases intersect. A corner vertex is interpolated. The contribution to the volume by a facet adjacent to a dart, or corner vertex is determined by yet other trilinear forms. The forms depend on the valence of the vertex and require an enumeration alike the one carried out in the previous chapter.

References

- [Autodesk 2013] Polson B., van Gelder D., Kraemer M., Ruffolo D., Tejima T.: *Meet the Experts: Pixar Animation Studios, The OpenSubdiv Project*, <https://www.youtube.com/watch?v=xFZazwvYc5o>, 2013
- [Catmull/Clark 1978] Catmull E., Clark J.: *Recursively generated B-spline surfaces on arbitrary topological meshes*, *Computer-Aided Design* 16(6), 1978
- [DeRose et al. 1998] DeRose T., Kass M., Truong T.: *Subdivision Surfaces in Character Animation*, SIGGRAPH '98, p. 85-94, 1998
- [Hakenberg et al. 2014] Hakenberg J., Reif U., Schaefer S., Warren J.: *Volume Enclosed by Subdivision Surfaces*, <http://vixra.org/abs/1405.0012>, 2014
- [Hakenberg 2014] Hakenberg J.: *Volume Enclosed by Example Subdivision Surfaces with Sharp Creases*, <http://vixra.org/abs/1405.0324>, 2014
- [Hoppe et al. 1994] Hoppe H., DeRose T., Duchamp T., Halstead M., Jin H., McDonald J., Schweitzer J., Stuetzle W.: *Piecewise smooth surface reconstruction*, *Computer Graphics*, 28(3):295-302, July 1994
- [Loop 1987] Loop C.: *Smooth subdivision surfaces based on triangles*, Master's thesis, University of Utah, 1987

Appendix: The volume enclosed by the first subdivision surface exhibited in the figure on page 1 is the fraction

```
438480126765110801308713852870154464426614320277848387707633988369003747617607671897425132092602393733716543587001237883990887450630233981387635306984525932432032477697090392988
2974977531246894907380493554660632866874594913035539311278214515092376584920822123356621654306444481255146092855885198730304671645582858152271629963247967499629314024851046447586
493812717634864572333199120310964833749732469540497647303696116316577039141147433411400845044158118840389373619361652871551245078590622631457462008062531328283720110283065649262
8393335440034919160469153878700096287454376127394966444157065432108731637424647494711306849098277352554709072381531021631104694280867445889047470654724027963065037177675785775426
9803624268203929792287309757484769832006750910985381354750855599347 /
1480562179208902579220597578594113317213432494229283759290852119556056793277955159197158452630196167226260606137059607741271531291040832055082790314320656104135550825401620530178
7773563415223720226833355970572281028440741969595881901363578891817567887214774538426410039336535928004737875420596658451386148540261379981414353029180263984065718043441822170108
8869546504100938928506360650941767433358421625760825668708596154140222890251423421528731328156540113601453959509947750072745643901662757187449238675753506723729417587449470047007
73131811279987781247030522569475363723125897821700161190800044798153723976011795420639876826544444475283276464220000974144449526422930163876440011119010853796175269015936820475266
51810008298294765822557770795229429130534819559753759848857600000.
```